LAWRENCE
LIVERMORE
NATIONAL
LABORATORY

UCRL-TR-233202

Estimate of the 9Be(n,el) Cross-section Uncertainties for the ENDL99 and ENDF/B-VII Evaluations

W. Younes, J. Pruet

July 31, 2007

This work was performed under the auspices of the U.S. Department of Energy by University of California, Lawrence Livermore National Laboratory under Contract W-7405-Eng-48.

Estimate of the $^{9}\mathrm{Be}\,(n,\mathrm{el})$ cross-section uncertainties for the ENDL99 and ENDF/B-VII evaluations

W. Younes and J. Pruet

Lawrence Livermore National Laboratory, Livermore, California 94551

(Dated: 30th July 2007)

Abstract

Uncertainties for the ENDL99 and ENDF/B-VII evaluations of the $^{9}\mathrm{Be}\,(n,\mathrm{el})$ cross section have been estimated for incident neutron energies up to 20 MeV. The uncertainties were obtained by extracting the spread of the experimental data about the evaluations, using a sophisticated procedure to ensure smoothness of the uncertainty as a function of energy. The technique used to obtain the uncertainties is described briefly in this report, and the resulting error bands are given for the two evaluations.

The uncertainty in the $^{9}\mathrm{Be}\,(n,\mathrm{el})$ cross section reported here has interesting implications for studies involving measured critical assemblies. Assemblies reflected by beryllium are useful in part because scattering from this light nucleus leads to a spectrum that is appreciably softer than the spectrum present in a bare-metal assembly. In principle, measured k eigenvalues for these critical assemblies could be used to get information about fission involving the relatively soft neutrons.

A technique for assigning uncertainties to data evaluations was presented in [1]. Rather than relying on variations of a parameterized model against experimental data to estimate the uncertainty in the evaluation, the technique described in [1] constructs an error band that reflects the spread of experimental measurements about the evaluation curve. It was argued in [1] that this technique avoids the pitfalls and limitations of varying a model that does not generally have complete or even correct physics, and where some aspects of the model cannot be varied in the continuous manner required to extract a proper model uncertainty (e.g., "variations" of the discrete level scheme in a Hauser-Feshbach cross-section calculation).

For the $^{9}\mathrm{Be}\,(n,\mathrm{el})$ cross section, experimental data from the EXFOR/CSISRS database were used [5]. The uncertainty-band construction procedure used in this work requires that the experimental data carry a y-error bar. Based on this criterion, several data points provided for the $^{9}\mathrm{Be}\,(n,\mathrm{el})$ cross section in the EXFOR/CSISRS database had to be discarded. The final data sets used in our analysis are listed in table I. In all, 109 experimental data points spanning the incident-neutron energy range $E_n = 0.03 - 21.6$ MeV were selected. As required by the uncertainty-band construction method [1], a set of points was sampled by a Monte-Carlo procedure from the 109 experimental measurements and their associated uncertainties [6]. A set of $N = 326689$ Monte-Carlo points was generated from the experimental data with a number of samples for each data point proportional to the inverse-variance associated with that data point [7].

Starting from the set of Monte-Carlo points, the uncertainty-band construction algorithm breaks up the entire energy range covered by the evaluation curve into intervals. within each interval, a symmetric band is expanded gradually about the evaluation curve, assuming the uncertainty is a constant over the interval, until 68.269% of the Monte-Carlo points encompassed by the interval are included within the band. In principle, this approach yields a band that represents the one-standard-deviation of the experimental data from the evaluation curve, assuming that the uncertainty is a slowly-varying function of the

energy. The outstanding question that remains to be answered is how to best choose the energy intervals used by the algorithm. In [1], the intervals were chosen so that each would encompass a statistically-significant subset of the Monte-Carlo points. Although this is a reasonable criterion, it does not guarantee that the resulting uncertainty will be a slowly-varying function of energy. Since the slowly-varying character of the uncertainty function is a necessary condition for the band-construction algorithm to perform correctly, it is not sufficient to merely ensure that the number of Monte-Carlo points within each interval is statistically significant.

Even though the algorithm assumes the uncertainty function is constant within each interval, it can be shown [3] that the band-construction algorithm will work very well if the uncertainty varies linearly with energy within each interval, provided the slope of the line is not too steep. Quantitatively, for an interval $[x_0 - \Delta x/2, x_0 + \Delta x/2]$ about x_0, a slope of b for the linear uncertainty function, and a value of $\sigma_y(x)$ for the uncertainty function at x, the algorithm will work well as long as the quantity

$$\rho \equiv \left| \frac{b\Delta x}{\sigma_y(x_0)} \right| \tag{1}$$

is not much greater than 1, and preferably as small as possible [3]. Thus, a procedure for selecting appropriate intervals suggests itself. First, within each interval, the values of the uncertainty function $\sigma_y(x)$ are fit with a straight line $s_y(x) = a + bx$, and the interval sizes are adjusted until all the relative residuals

$$r(x) \equiv \left| \frac{\sigma_y(x) - s_y(x)}{\sigma_y(x_0)} \right| \tag{2}$$

are smaller than some user-defined limit, ε_{lin}, which should be small compared to 1. This step ensures that the uncertainty is an approximately linear function of x. Then, while still keeping $r(x) \leq \varepsilon_{lin}$, the intervals are further adjusted to reduce the relative slope, ρ, given by Eq. (1). In practice, the intervals are initially chosen so that they contain a minimum number N_{min} of Monte-Carlo points. Then the intervals are either expanded or reduced in small increments to minimize ρ while satisfying $r(x) \leq \varepsilon_{lin}$.

The approach described above has been applied to the ENDL99 evaluation [8] of the ^{9}Be(n, el) cross section. Initial sizes for the energy intervals were chosen so that each contained at least $N_{min} = 30000$ points (or $\approx 9.2\%$ of the total number of Monte-Carlo points). The intervals were then adjusted to linearize the uncertainty function with $\varepsilon_{lin} = 0.2$, and

then further adjusted to minimize the relative slope ρ. A final upper bound of $\rho \leq 0.9554$ was attained for all intervals. The resulting uncertainty function is displayed in Fig. 1, and listed for easy reference in Table II. The linearity and low-slope conditions imposed above were introduced to ensure internal consistency of the band-construction method, but they also serve to keep the uncertainties relatively small, even in energy regions where the data have larger error bars. This can be seen in the top panel of Fig. 1, where the experimental points at the lowest energies ($E_n \gtrsim 0.03$ MeV) carry $\sim$10% uncertainties but the error band, whose width is constrained to vary slowly with energy, is influenced by better-measured data at higher energies and maintains a $\lesssim 5\%$ uncertainty level. The bottom panel in Fig. 1 shows the deduced relative uncertainty for the ENDL99 evaluation, which is generally better that $\sim$5%, with two notable exceptions. Near $E_n \approx 2$ MeV, the uncertainty rises to $\sim$10% because of a lack of experimental data in the range $E_n = 1.4 - 2.5$ MeV. The relative uncertainty also rises near $E_n = 20$ MeV, because the cross section section is dropping at those higher energies, and there is some disagreement between the evaluation and the data in that region.

The deduced uncertainty band for the ENDF/B-VII evaluation is shown in Fig. 2, and listed in Table III [9]. For this case, an initial number $N_{min} = 25000$ of points in each interval (or $\approx 7.7\%$ of the total number of Monte-Carlo points) was used, and the intervals were adjusted with $\varepsilon_{lin} = 0.25$, and a final upper bound for the relative slope of $\rho \leq 1.1303$. The deduced relative uncertainty shown in the bottom panel of Fig. 2, is similar to the result obtained for the ENDL99 evaluation. The uncertainty is slightly larger near $E_n \approx 6.6$ and 10.7 MeV than for the ENDL99 evaluation, but smaller near $E_n = 20$ MeV, where the ENDF/B-VII evaluation follows the experimental data better.

In this report, we provide estimated errors for the ENDL99 and ENDF/B-VII evaluations of the ^{9}Be$\,(n, \mathrm{el})$ cross section up to $E_n = 20$ MeV. The uncertainties have been obtained using a sophisticated algorithm that measures the spread of the experimental data about the evaluation. In the future, the algorithm could be improved, so that a smaller initial intervals could be used as a starting points (i.e., smaller values of N_{min}), while still converging to a solution with more linear behavior of the uncertainty function in each energy interval (i.e., smaller values of ε_{lin}), and a lower slope for the lines in each interval (i.e., a smaller upper bound for ρ). It is not expected that such an improved algorithm would lead to a deduced uncertainties significantly different from the ones reported here. Our estimates indicate that

uncertainties in the $^{9}\mathrm{Be}\,(n,\mathrm{el})$ cross section are too large to allow strong inferences about fission with soft neutrons. This is illustrated in figure 3, which shows the prompt k eigenvalue for a beryllium-reflected assembly as a function of the percent change in the $^{9}\mathrm{Be}\,(n,\mathrm{el})$ cross section. The change in the k eigenvalue is approximately

$$\delta k \;\approx\; 0.01 \cdot \frac{\delta\sigma\,(n,\mathrm{el})}{5\%}$$

This report found that for fission spectrum neutrons the uncertainty in the Be(n,el) cross section ranges from approximately 4% to approximately 10%. A 5% uncertainty in the elastic cross section implies an uncertainty in k of approximately 0.01, which is some three times larger than the experimental uncertainty of 0.003 in the k eigenvalue. Even fairly large discrepancies between calculations and experiments for this assembly can be be explained in terms of errors in cross sections involving Be rather than in the treatment of reactions involving plutonium and low energy neutrons.

EXFOR/CSISRS label	Included?	Comments
10550004	yes	
10678005	yes	
11192003	yes	
11201003	no	no error bars given
11207002	yes	
11214003	no	no y-error bars given
11215002	yes	
11224002	yes	
11228002	yes	
11232002	yes	
11237003	yes	some points excluded because of no y-error bars
11251004	no	no error bars given
12939005	yes	
13154004	yes	
20599002	yes	
20872002	yes	
21177011	yes	
22113010	yes	
22127002	yes	
30623005	yes	
40221003	yes	
78009003	yes	

Table I: Summary of experimental data used in the present analysis. The identifying label for the data taken from the EXFOR/CSISRS database is given in the first column. The second column states whether the data set was used in the analysis or discarded. The third column provides a justification wherever part or all of a data set was discarded.

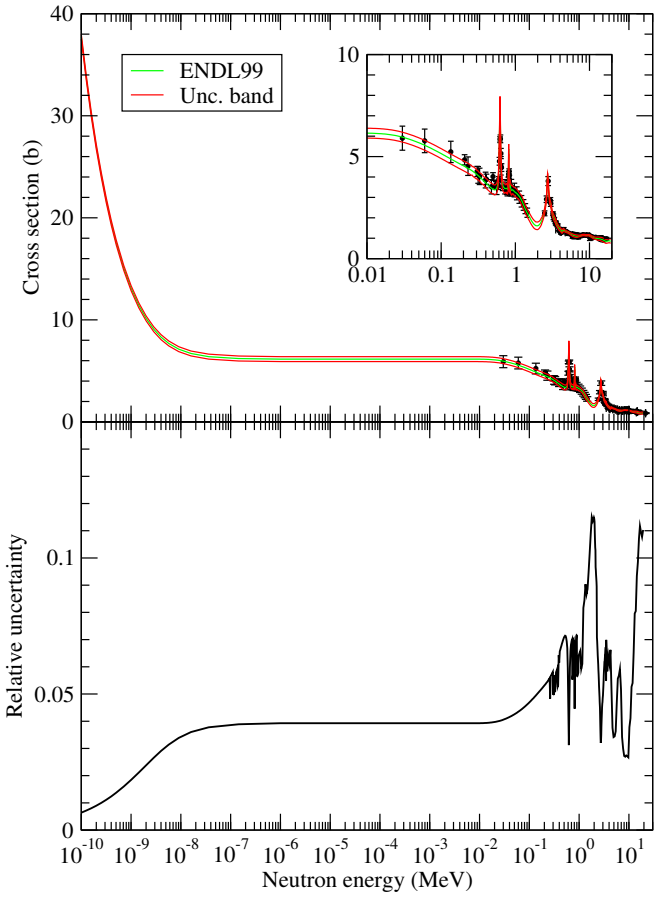

Figure 1: Deduced uncertainty band for the ENDL99 evaluation. The top panel shows the evaluation (green line), experimental data, and uncertainty band (red lines on either side of the evaluation curve) as a function of incident neutron energy. The inset gives a close-up view in the reduced energy range $E_n = 0.01 - 20$ MeV. The bottom panel shows the corresponding relative uncertainty.

Table II: Tabulated relative uncertainties for the ENDL99 evaluation. Note that the point at $E_n = 3.6$ MeV has a higher relative uncertainty than what is plotted in Fig. 1 because the curves in the figure are splined and plotted for slightly different energies than the original ENDL99 evaluation.

E_n (MeV)	Cross section (b)	Relative uncertainty
1.000×10^{-10}	37.762	0.0064
1.260×10^{-10}	33.745	0.0072
1.587×10^{-10}	30.177	0.0080
1.999×10^{-10}	27.012	0.0089
2.517×10^{-10}	24.206	0.0100
3.171×10^{-10}	21.723	0.0111
3.994×10^{-10}	19.528	0.0124
5.031×10^{-10}	17.592	0.0137
7.160×10^{-10}	15.075	0.0160
1.005×10^{-9}	13.092	0.0184
1.431×10^{-9}	11.420	0.0211
2.009×10^{-9}	10.134	0.0238
2.860×10^{-9}	9.081	0.0266
4.016×10^{-9}	8.300	0.0291
5.715×10^{-9}	7.688	0.0314
9.068×10^{-9}	7.129	0.0339
1.604×10^{-8}	6.705	0.0360
3.622×10^{-8}	6.396	0.0378
1.447×10^{-7}	6.212	0.0389
2.954×10^{-3}	6.150	0.0393
3.721×10^{-3}	6.150	0.0393
9.146×10^{-3}	6.150	0.0393
3.582×10^{-2}	5.870	0.0411
2.531×10^{-1}	4.336	0.0567
5.000×10^{-1}	3.400	0.0709
5.647×10^{-1}	3.481	0.0692
5.719×10^{-1}	3.538	0.0681
5.898×10^{-1}	3.946	0.0610
6.006×10^{-1}	4.688	0.0514
6.096×10^{-1}	5.945	0.0406
6.167×10^{-1}	7.380	0.0330
6.220×10^{-1}	7.698	0.0313
6.268×10^{-1}	7.255	0.0340
6.315×10^{-1}	6.470	0.0394
6.398×10^{-1}	4.641	0.0497
6.505×10^{-1}	4.086	0.0582
6.600×10^{-1}	3.820	0.0628
6.712×10^{-1}	3.644	0.0662
7.275×10^{-1}	3.431	0.0567
7.655×10^{-1}	3.434	0.0700
7.965×10^{-1}	3.530	0.0680
8.004×10^{-1}	3.638	0.0647
8.043×10^{-1}	4.025	0.0593
8.120×10^{-1}	5.440	0.0444
8.149×10^{-1}	4.911	0.0487
8.201×10^{-1}	3.698	0.0649
8.267×10^{-1}	3.483	0.0693
1.000×10^{0}	3.250	0.0646
1.200×10^{0}	2.900	0.0769
1.350×10^{0}	2.465	0.0905
1.500×10^{0}	2.130	0.0903
1.800×10^{0}	1.670	0.1151

continued on next page

Table II: *continued*

E_n (MeV)	Cross section (b)	Relative uncertainty
2.000×10^{0}	1.610	0.1146
2.250×10^{0}	1.830	0.0910
2.550×10^{0}	2.600	0.0500
2.600×10^{0}	2.810	0.0463
2.650×10^{0}	3.160	0.0411
2.700×10^{0}	3.920	0.0332
2.725×10^{0}	4.059	0.0320
2.800×10^{0}	3.470	0.0374
3.030×10^{0}	2.575	0.0505
3.100×10^{0}	2.360	0.0551
3.350×10^{0}	1.965	0.0648
3.600×10^{0}	1.700	0.1097
3.900×10^{0}	1.480	0.0678
4.160×10^{0}	1.305	0.0633
4.170×10^{0}	1.290	0.0638
4.300×10^{0}	1.390	0.0650
4.400×10^{0}	1.420	0.0573
4.625×10^{0}	1.365	0.0402
5.250×10^{0}	1.270	0.0345
5.500×10^{0}	1.220	0.0383
7.500×10^{0}	1.120	0.0304
8.400×10^{0}	1.160	0.0270
9.100×10^{0}	1.140	0.0276
9.500×10^{0}	1.150	0.0260
1.025×10^{1}	1.117	0.0380
1.100×10^{1}	1.050	0.0464
1.350×10^{1}	0.974	0.0799
1.600×10^{1}	0.872	0.1083
1.650×10^{1}	0.846	0.1114
1.800×10^{1}	0.873	0.1079
2.000×10^{1}	0.843	0.1052

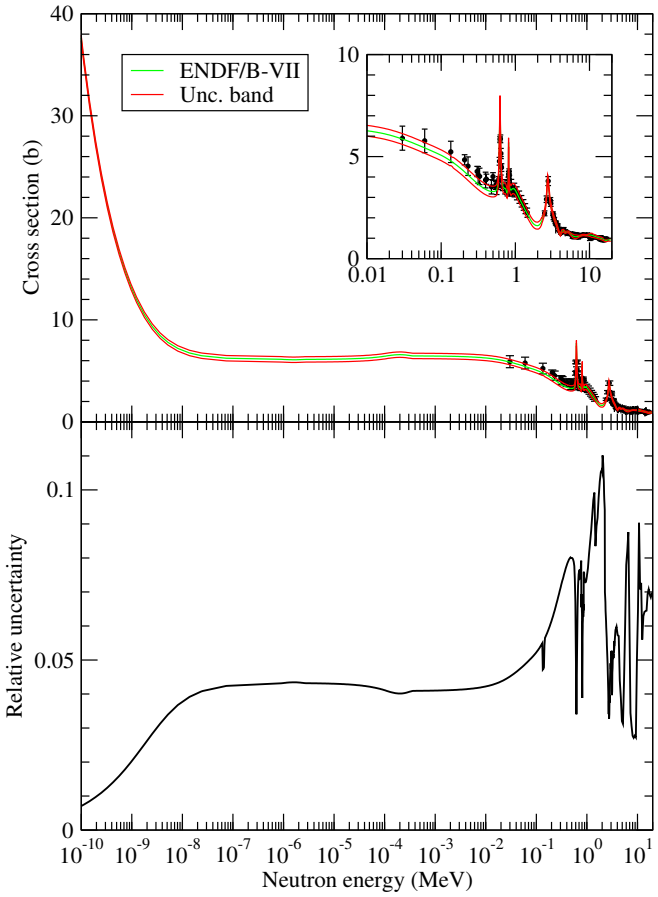

Figure 2: Same as Fig. 1, but for the ENDF/B-VII evaluation.

Table III: Tabulated relative uncertainties for the ENDF/B-VII evaluation.

E_n (MeV)	Cross section (b)	Relative uncertainty
1.000×10^{-11}	117.301	0.0023
1.312×10^{-11}	102.429	0.0026
1.709×10^{-11}	89.808	0.0029
2.243×10^{-11}	78.442	0.0034
2.920×10^{-11}	68.799	0.0038
3.832×10^{-11}	60.118	0.0044
4.989×10^{-11}	52.756	0.0050
6.548×10^{-11}	46.133	0.0057
8.526×10^{-11}	40.522	0.0065
1.119×10^{-10}	35.478	0.0075
1.457×10^{-10}	31.212	0.0085
1.912×10^{-10}	27.384	0.0097
2.489×10^{-10}	24.153	0.0110
3.267×10^{-10}	21.264	0.0124
4.254×10^{-10}	18.835	0.0140
5.583×10^{-10}	16.674	0.0159
7.269×10^{-10}	14.870	0.0178
9.539×10^{-10}	13.278	0.0199
1.242×10^{-9}	11.962	0.0221
1.775×10^{-9}	10.497	0.0252
2.537×10^{-9}	9.345	0.0283
3.627×10^{-9}	8.458	0.0313
5.183×10^{-9}	7.791	0.0340
8.133×10^{-9}	7.198	0.0368
1.390×10^{-8}	6.753	0.0392
2.347×10^{-8}	6.496	0.0407
2.530×10^{-8}	6.469	0.0409
7.387×10^{-8}	6.241	0.0424
9.002×10^{-7}	6.132	0.0431
2.885×10^{-6}	6.127	0.0432
1.089×10^{-4}	6.463	0.0409
3.797×10^{-4}	6.464	0.0409
2.243×10^{-2}	6.008	0.0440
1.000×10^{-1}	5.064	0.0523
2.500×10^{-1}	3.978	0.0665
5.000×10^{-1}	3.285	0.0800
5.525×10^{-1}	3.343	0.0787
5.750×10^{-1}	3.511	0.0747
5.850×10^{-1}	3.717	0.0712
5.900×10^{-1}	3.855	0.0683
6.000×10^{-1}	4.483	0.0583
6.100×10^{-1}	5.989	0.0442
6.162×10^{-1}	7.318	0.0365
6.188×10^{-1}	7.645	0.0347
6.200×10^{-1}	7.747	0.0342
6.240×10^{-1}	7.468	0.0348
6.312×10^{-1}	6.144	0.0424
6.400×10^{-1}	4.834	0.0543
6.500×10^{-1}	4.148	0.0633
6.636×10^{-1}	3.758	0.0700
6.700×10^{-1}	3.653	0.0720
7.000×10^{-1}	3.450	0.0760
7.500×10^{-1}	3.367	0.0756
7.937×10^{-1}	3.375	0.0659
8.000×10^{-1}	3.483	0.0636
8.050×10^{-1}	4.028	0.0550
8.100×10^{-1}	5.795	0.0383
8.125×10^{-1}	5.329	0.0415

continued on next page

Table III: *continued*

E_n (MeV)	Cross section (b)	Relative uncertainty
8.150×10^{-1}	4.589	0.0483
8.200×10^{-1}	3.940	0.0562
8.250×10^{-1}	3.716	0.0596
8.300×10^{-1}	3.614	0.0613
9.000×10^{-1}	3.404	0.0737
1.075×10^{0}	3.131	0.0788
1.500×10^{0}	2.096	0.0832
1.749×10^{0}	1.709	0.1003
1.880×10^{0}	1.628	0.1052
2.000×10^{0}	1.618	0.1058
2.100×10^{0}	1.655	0.1078
2.250×10^{0}	1.815	0.0960
2.440×10^{0}	2.199	0.0581
2.562×10^{0}	2.602	0.0488
2.600×10^{0}	2.800	0.0454
2.663×10^{0}	3.382	0.0381
2.700×10^{0}	3.815	0.0346
2.725×10^{0}	3.971	0.0379
2.763×10^{0}	3.863	0.0320
2.900×10^{0}	3.030	0.0470
3.100×10^{0}	2.423	0.0524
3.300×10^{0}	2.033	0.0506
3.550×10^{0}	1.732	0.0546
4.200×10^{0}	1.262	0.0581
4.300×10^{0}	1.402	0.0549
4.450×10^{0}	1.380	0.0449
4.800×10^{0}	1.277	0.0359
5.000×10^{0}	1.320	0.0305
5.500×10^{0}	1.220	0.0476
7.500×10^{0}	1.120	0.0306
8.400×10^{0}	1.160	0.0270
9.100×10^{0}	1.140	0.0254
9.500×10^{0}	1.150	0.0369
1.310×10^{1}	1.031	0.0633
1.460×10^{1}	0.983	0.0643
1.650×10^{1}	0.892	0.0709
1.800×10^{1}	0.923	0.0684
2.000×10^{1}	0.895	0.0671

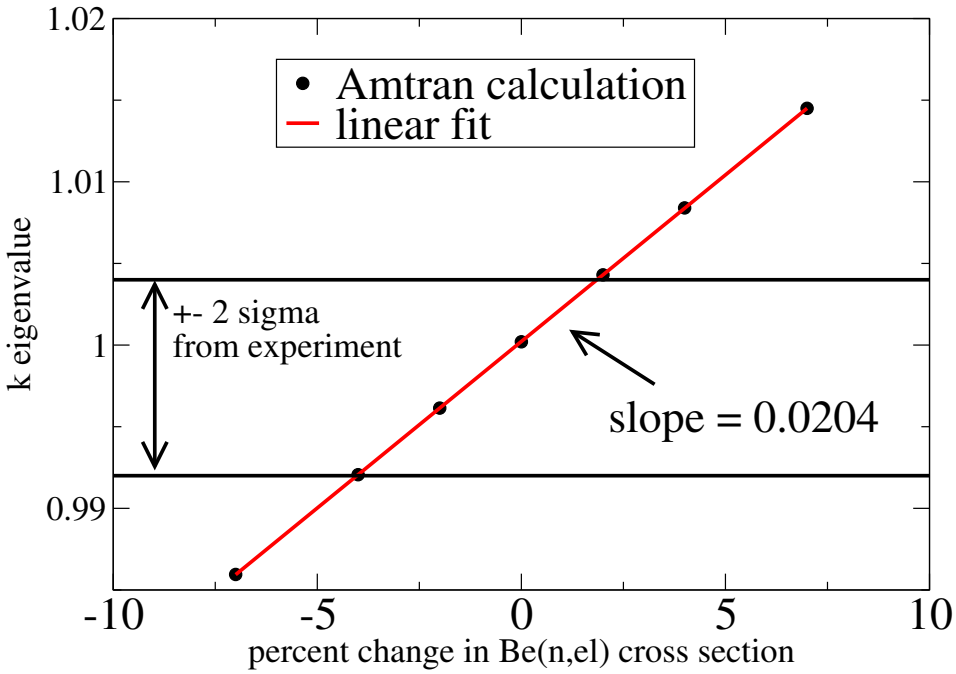

Figure 3: Relation between the k eigenvalue for a Be-reflected assembly and the Be (n, el) cross section. The assembly, Pu-MET-FAT-018, is a plutonium metal sphere surrounded by approximately 3.7 cm of beryllium (see [4] for a discussion of experiments and evaluations for this assembly). The experimental prompt k eigenvalue for Pu-MET-FAST-018 is $k = 0.998 \pm 0.003$, where we have taken the contribution of β-delayed neutrons to be the same as for the bare Jezebel assembly. Note that changes in the Be (n, el) cross section of order 5% (the approximate size of uncertainties estimated in this report) result in changes in k which are much larger than the experimental uncertainties in k. Amtran is a Livermore S_n code.

---

[1] W. Younes, "A Systematic Procedure for Assigning Uncertainties to Data Evaluations.", LLNL Tech. Rep. UCRL-TR-228283 (2007).

[2] W. H. Press, *et al.*, *Numerical Recipes in C: the Art of Scientific Computing*, 2nd Ed., p. 666, Cambridge University Press, Cambridge (2002).

[3] W. Younes, internal report in preparation.

[4] NEA Nuclear Science Committee 1998, "International Handbook of Evaluated Criticality Safety Benchmark Experiments", NEA/NSC/DOC (95)03, 1998 edition.

[5] Data from the EXFOR/CSISRS database were downloaded from the LLNL Nuclear and Atomic Database System (NADS) at "nuclear.llnl.gov/CNP/nads/NADSApplet.html".

[6] This Monte-Carlo sampling is performed to treat x- and y-error bars in the data on an equal footing.

[7] The inverse-variance weighting of the experimental data was used as a standard method for reducing bias in estimations based on these data. For data points with both x- and y-error bars, the two were combined in quadrature, using the slope of the evaluation curve to scale the x-error value (see [2]).

[8] The ENDL99 evaluation was downloaded from the LLNL Nuclear and Atomic Database System (NADS) at "nuclear.llnl.gov/CNP/nads/NADSApplet.html".

[9] The ENDF/B-VII evaluation was downloaded from the LLNL Nuclear and Atomic Database System (NADS) at "nuclear.llnl.gov/CNP/nads/NADSApplet.html".